university of groningen

University Medical Center Groningen

University of Groningen

Proximity induced room temperature ferromagnetism in graphene probed with spin currents

Leutenantsmeyer, Johannes Christian; Kaverzin, Alexey A.; Wojtaszek, Magdalena; van Wees, Bart J.

Published in:
2D Materials

DOI:
10.1088/2053-1583/4/1/014001

IMPORTANT NOTE: You are advised to consult the publisher's version (publisher's PDF) if you wish to cite from it. Please check the document version below.

Document Version
Publisher's PDF, also known as Version of record

Publication date:
2017

Link to publication in University of Groningen/UMCG research database

Citation for published version (APA):
Leutenantsmeyer, J. C., Kaverzin, A. A., Wojtaszek, M., & van Wees, B. J. (2017). Proximity induced room temperature ferromagnetism in graphene probed with spin currents. *2D Materials*, *4*(1), [014001]. https://doi.org/10.1088/2053-1583/4/1/014001

Copyright
Other than for strictly personal use, it is not permitted to download or to forward/distribute the text or part of it without the consent of the author(s) and/or copyright holder(s), unless the work is under an open content license (like Creative Commons).

The publication may also be distributed here under the terms of Article 25fa of the Dutch Copyright Act, indicated by the "Taverne" license. More information can be found on the University of Groningen website: https://www.rug.nl/library/open-access/self-archiving-pure/taverne-amendment.

Take-down policy
If you believe that this document breaches copyright please contact us providing details, and we will remove access to the work immediately and investigate your claim.

Downloaded from the University of Groningen/UMCG research database (Pure): http://www.rug.nl/research/portal. For technical reasons the number of authors shown on this cover page is limited to 10 maximum.

Download date: 05-05-2023

PAPER • **OPEN ACCESS**

Proximity induced room temperature ferromagnetism in graphene probed with spin currents

To cite this article: Johannes Christian Leutenantsmeyer *et al* 2017 *2D Mater.* **4** 014001

View the article online for updates and enhancements.

Related content

- Spin precession and spin Hall effect in monolayer graphene/Pt nanostructures
W Savero Torres, J F Sierra, L A Benítez et al.
- Spin diffusion and non-local spin-valve effect in an exfoliated multilayer graphene with a Co electrode
Lijun Li, Inyeal Lee, Dongsuk Lim et al.
- Electrical spin injection, transport, and detection in graphene-hexagonal boron nitride van der Waals heterostructures: progress and perspectives
M Gurram, S Omar and B J van Wees

Recent citations

- Spin-dependent quantum beating of the conductance oscillations in asymmetric velocity modulated ferromagnetic graphene junction
Chaiyawan Saipaopan *et al*
- Spin-Split Band Hybridization in Graphene Proximitized with -RuCl3 Nanosheets
Soudabeh Mashhadi *et al*
- Valley-Mediated and Electrically Switched Bipolar-Unipolar Transition of the Spin-Diode Effect in Heavy Group-IV Monolayers
Xuechao Zhai *et al*

This content was downloaded from IP address 129.125.136.115 on 16/09/2019 at 12:40

2D Materials

OPEN ACCESS

RECEIVED
11 October 2016

ACCEPTED FOR PUBLICATION
21 October 2016

PUBLISHED
4 November 2016

Original content from this work may be used under the terms of the Creative Commons Attribution 3.0 licence.

Any further distribution of this work must maintain attribution to the author(s) and the title of the work, journal citation and DOI.

PAPER

Proximity induced room temperature ferromagnetism in graphene probed with spin currents

Johannes Christian Leutenantsmeyer[1], **Alexey A Kaverzin**[1], **Magdalena Wojtaszek and Bart J van Wees**

Physics of Nanodevices, Zernike Institute for Advanced Materials, University of Groningen, 9747 AG Groningen, The Netherlands

[1] These authors contributed equally to this work.

E-mail: j.c.leutenantsmeyer@rug.nl

Keywords: graphene, proximity induced magnetization, spintronics

Supplementary material for this article is available online

Abstract

We present a direct measurement of the exchange interaction in room temperature ferromagnetic graphene. We study the spin transport in exfoliated graphene on an yttrium–iron–garnet substrate where the observed spin precession clearly indicates the presence and strength of an exchange field that is an unambiguous evidence of induced ferromagnetism. We describe the results with a modified Bloch diffusion equation and extract an average exchange field of the order of 0.2 T. Further, we demonstrate that a proximity induced 2D ferromagnet can efficiently modulate a spin current by controlling the direction of the exchange field. These findings can create a building block for magnetic-gate tuneable spin transport in one-atom-thick spintronic devices.

The introduction and control of ferromagnetism in graphene opens up a range of new directions for fundamental and applied studies [1, 2]. Several approaches have been pursued so far, such as introduction of defects, functionalisation with adatoms, and shaping of graphene into nanoribbons with well-defined zigzag edges [3–8]. A more robust and less invasive method utilises the introduction of an exchange interaction by a ferromagnetic insulator (FMI) in proximity with graphene [9–16]. The magnetic proximity effect describes the introduction of ferromagnetic order into an intrinsically nonmagnetic material by an adjacent ferromagnet due to the exchange interaction between the spins in the magnetic and non-magnetic material. Being atomically thin, graphene presents an ideal platform for studying such interaction, in particular when combined with a FMI. Theory predicts that for the idealised case of (super) lattice matching an exchange splitting of tens of meV can be obtained [16]. Up to date it has been studied experimentally in a number of FMI/graphene systems using materials with low Curie temperature such as EuO ($T_c = 69$ K) and EuS ($T_c = 16.5$ K) [13, 14]. In comparison, yttrium–iron–garnet (YIG) provides the advantage of a Curie temperature of 550 K, along with chemical stability in atmospheric conditions, the preservation of the charge transport properties in the graphene and the possibility to directly exfoliate or transfer graphene onto the surface for fabricating graphene-based spintronic devices.

As indication of a ferromagnetic exchange interaction in graphene/YIG heterostructures the observation of an anomalous Hall effect was reported [9]. More recently, the presence of an exchange interaction in YIG/CVD graphene devices was invoked to explain magnetoresistance measurements and ferromagnetic resonance spin pumping [15]. So far, in all the reports the authors employ charge transport, where in addition to exchange interaction also spin–orbit interaction is needed for the understanding, both *a priori* unknown parameters.

In this work, we probe the induced exchange interaction in graphene in the most direct way using only the spin degree of freedom. The magnetic interaction between the YIG magnetisation and the graphene spins is expected to produce an exchange term in the Hamiltonian and to spin split the graphene energy bands (figure 1(a)). It can be described as an additional effective exchange field that is determined by the direction and magnitude of the YIG magnetisation. By studying its effect on spin transport and precession, and fitting the results with the modified Bloch spin diffusion equation we are able to describe our results qualitatively and quantitatively. We further

© 2016 IOP Publishing Ltd

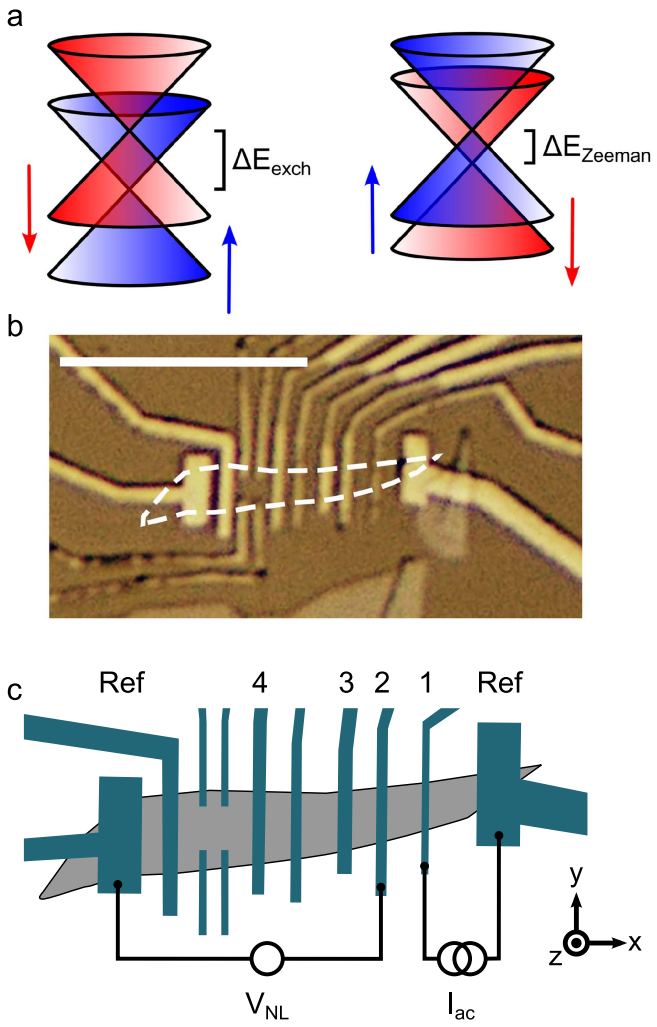

Figure 1. Spin transport in graphene in the presence of a proximity induced exchange field. (a) The exchange field creates a splitting of the Dirac cone for each spin species similar to the magnetic field induced Zeeman splitting. Note that both the sign and magnitude of the exchange and Zeeman splitting can be different. (b) Optical micrograph of the graphene/YIG heterostructures indicating the single layer graphene flake and the deposited TiO_2/Co contacts. To control the coercive field of the electrodes for magnetisation switching, we define different contact widths between 200 and 400 nm. The scale bar represents 10 μm. (c) Schematic sketch of the sample showing the characterised injector/detector contacts (1, 2, 3, 4) and reference contacts (Ref). The circuit for the measurements shown in figures 2 and 3 is indicated.

demonstrate that the precession induced by the exchange field can be used for an efficient modulation of spin currents.

The device is shown in figures 1(b) and (c). A single layer graphene flake of approximately 12 μm by 1.2 μm is first exfoliated on SiO_2 and transferred to YIG. Ferromagnetic contacts are defined via e-beam lithography followed by Ti deposition, *in situ* oxidation to form TiO_2, Co deposition and liftoff. A non-local spin valve characterisation [17] is shown in figure 2. A charge current is sent from the injector to the reference electrode. As a result a pure spin current diffuses through the channel and is detected as a voltage difference between the detecting and another reference electrode. The spin-transport measurements are obtained using contacts 1 and 2 as injector and detector with contact spacing $d = 1.2$ μm. The magnetisation direction of the injector (detector) can be controlled by sweeping the applied magnetic field along the easy axis of the electrodes. Figure 2(b) shows the change of the non-local resistance (R_{NL}) when the electrode configuration is switched between parallel and antiparallel alignment. The change in R_{NL} is a pure spin signal that increases from 90 mΩ at room temperature to 650 mΩ at 75 K. To determine the spin relaxation length λ, we fit the dependence of the spin signal on d and extract $\lambda = (490 \pm 40)$ nm (see footnote 2). These values are comparable to our other graphene devices on YIG or SiO_2 [18], which confirms that the basic spin transport properties of graphene are conserved after transfer to YIG.

To investigate the presence of the exchange field, we study the Hanle spin precession (figure 3(a)). A perpendicular magnetic field causes injected spins to precess while diffusing along the channel, changing the average polarisation and direction of the spins at

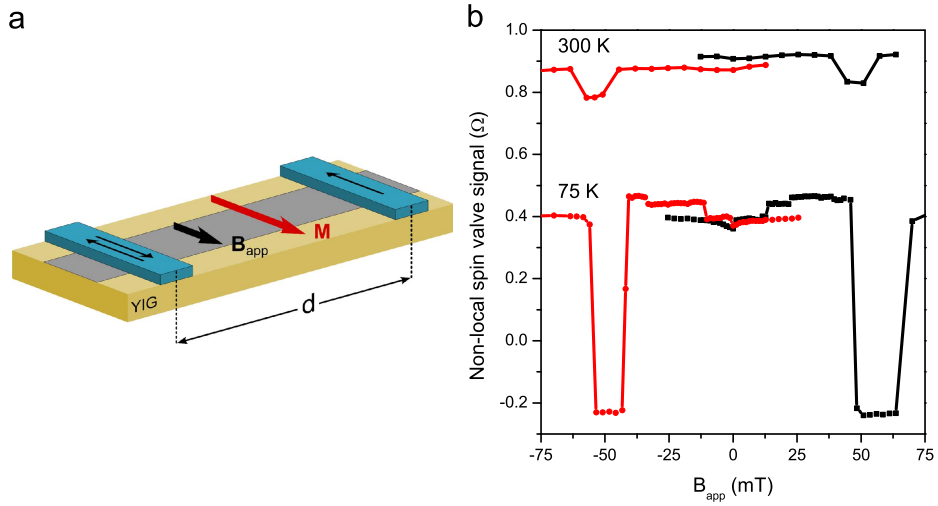

Figure 2. Non-local spin transport in graphene spin valves on YIG. (a) Schematic measurement to characterise the non-local spin transport by switching the electrode magnetisation with an external magnetic field ($\mathbf{B}_{app}$). **M** denotes the magnetisation of the YIG film and is parallel to $\mathbf{B}_{app}$ for these measurements. The exchange field is parallel or antiparallel to the spin accumulation and hence does not affect the spin transport for this type of experiment. (b) The experimental data of the spin valve switching at 300 and 75 K is measured with $d = 1.2\ \mu$m. The black squares (negative to positive) and the red circles (positive to negative) correspond to different sweep directions of $\mathbf{B}_{app}$. The other switches can be attributed to smaller contributions of the outer electrodes to the spin signal.

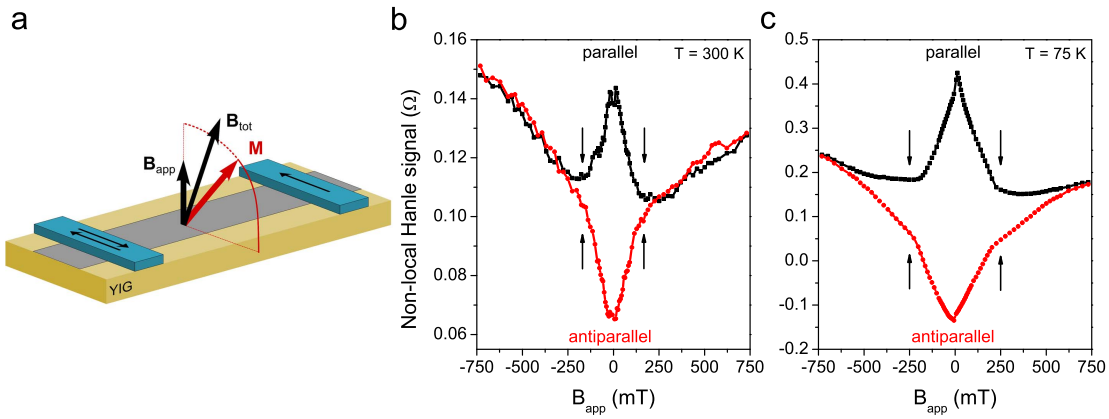

Figure 3. Hanle spin precession modified by the proximity induced exchange field. (a) The schematic measurement setup. $\mathbf{B}_{app}$ is applied perpendicular to plane. The total effective field $\mathbf{B}_{tot} = \mathbf{B}_{app} + \mathbf{B}_{exch}$ causes Hanle spin precession. (b) Non local resistance at room temperature and 75 K (c). The top curve (black squares) is measured with parallel injecting and detecting electrodes, the bottom curve (red circles) represents their antiparallel alignment. The black arrows indicate the perpendicular saturation field of the underlying YIG film.

the detector. The total effective field ($\mathbf{B}_{tot}$) that is sensed by the spins consists of the applied field ($\mathbf{B}_{app}$) and exchange field ($\mathbf{B}_{exch}$), $\mathbf{B}_{tot} = \mathbf{B}_{app} + \mathbf{B}_{exch}$. $\mathbf{B}_{app}$ is swept perpendicular to the sample plane and causes the Zeeman splitting of the graphene spins, $\Delta E_{Zeeman} = g\mu_B|\mathbf{B}_{app}|$. The exchange field is determined by the YIG magnetisation direction **M** and the interface properties and is defined as $\Delta E_{exch} = g\mu_B\ |\mathbf{B}_{exch}|$. Here g is the gyromagnetic factor (~2 for graphene) and μ_B the Bohr magnetron[2].

[2] Note that possible stray magnetic fields arising from the YIG magnetisation can be excluded. See the supplementary information for a detailed discussion.

Typical Hanle curves for graphene devices on SiO_2 [19] or hBN [20] substrates are smooth in the full measured range, whereas we clearly observe a sharp transition at $\mathbf{B}_{app} \sim 180$ mT in our sample. The kink is seen for both parallel and antiparallel injector/detector magnetisations at all measured temperatures although it becomes more pronounced at 75 K. The appearance of such transition requires an additional spin precession caused by the exchange field $\mathbf{B}_{exch}$ that is constant in magnitude and collinear with **M**. When no external field is applied, **M** together with $\mathbf{B}_{exch}$ lies within the sample plane and is gradually pulled out of the plane with increasing $\mathbf{B}_{app}$. The transition point coincides with the saturation field of the YIG

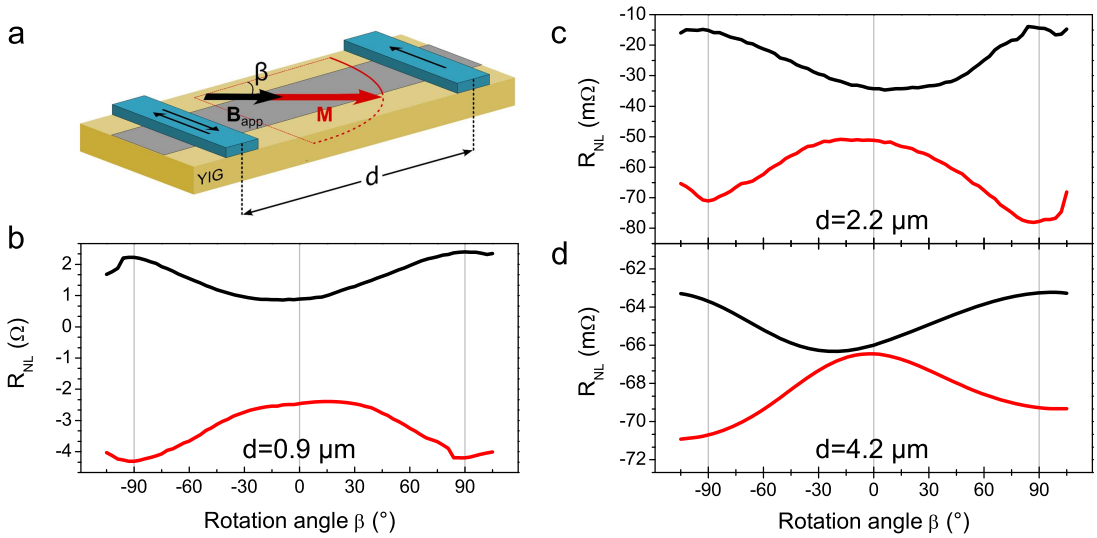

Figure 4. Spin transport modulated with an in-plane exchange field. (a) Schematic of the experiment. The YIG magnetisation is rotated with $|\mathbf{B}_{app}| = 20$ mT by an angle β in parallel (black) and antiparallel (red) electrode alignment. In this experiment only the exchange field causes significant spin precession, leading to a modulation of the spin signal. We show the modulation caused by the additional spin precession originating from the exchange field for three different distances (b)–(d), the full data set is shown in the supplementary information. For the farthest distance a smoothed curve is plotted. The relative modulation increases from 50% at $d = 0.9$ μm up to ~100% at $d = 4.2$ μm injector to detector spacing.

magnetisation ($\mathbf{B_s} \sim 180$ mT) above which $\mathbf{M}$ and $\mathbf{B}_{exch}$ are aligned fully perpendicular to the sample plane. The change of the transition field with temperature is consistent with the change of the magnetisation saturation field of the YIG films (see supplementary information). Thus, we conclude the existence of an exchange field and find a magnitude of about 0.2 T.

To further confirm the presence and magnitude of the exchange field, we utilise the low in-plane coercivity of YIG. By applying and rotating a small magnetic field of 20 mT in the sample plane we can control the magnetisation direction of the YIG without applying a significant spin precession with the applied field. Furthermore, we maintain the parallel/antiparallel alignment of the injector/detector electrodes (figure 4(a)), leaving the injected/detected spins unaffected. When $\mathbf{B}_{exch}$ is collinear with the injected spin polarisation ($\beta = \pm 90°$) it has no influence on the spin transport, whereas at $\beta = 0°$ the diffusing spins experience the maximum precession and dephasing. In figure 4(b) the dependence of the spin signal on β is shown for both parallel and antiparallel magnetisation alignment. For $d = 0.9$ μm (contacts 2 and 3, figure 1(c)) the observed modulation is around 50%, which is substantial and cannot be explained by the effect of $\mathbf{B}_{app}$(=20 mT) alone. With increasing distance between both electrodes the modulation reaches ~100% at $d = 4.2$ μm (figures 4(b)–(d)). In this case all spin components perpendicular to $\mathbf{B}_{exch}$ are dephased and averaged to zero and the spin signal has a dependence close to $\Delta R_{NL}(\beta) = \pm R^0_{NL} \cos^2 \beta$. These measurements confirm that the magnitude of the exchange field corresponds to approximately 0.2 T.

To model the spin transport in graphene in the presence of an exchange field, we add the exchange field to the one dimensional Bloch equation:

$$0 = D_s \nabla \boldsymbol{\mu}_s - \frac{\boldsymbol{\mu}_s}{\tau_s} + \frac{g\mu_B}{\hbar}(\mathbf{B}_{app} + \mathbf{B}_{exch}) \times \boldsymbol{\mu}_s,$$

where D_s denotes the spin diffusion coefficient, $\boldsymbol{\mu}_s$ the three-component spin chemical potential, τ_s the spin relaxation time and $\hbar$ the reduced Planck constant. We obtain an analytical expression for the spin accumulation at the detector depending on $\mathbf{B}_{app}$. Below the YIG saturation field $\mathbf{B}_s$ both $\mathbf{M}$ and $\mathbf{B}_{exch}$ are determined by the standard easy-plane magnetic anisotropy model, whereas above the saturation field $\mathbf{B}_{exch}$ is fixed and aligned with $\mathbf{B}_{app}$ (see footnote 2). We use our model to qualitatively reproduce the observed behaviour and also make a quantitative estimation of the exchange field. The fitting of the Hanle curve is shown in figures 5(a), (b), where we find the best agreement for $\lambda = 1.8$ μm ($\lambda = \sqrt{D_s \tau_s}$) and $|\mathbf{B}_{exch}| = 0.2$ T. A possible explanation for the difference between λ extracted from the distance dependent spin signal ($\lambda = 490$ nm) and from the modelling ($\lambda = 1.8$ μm) is a spatial inhomogeneity of the exchange field. $|\mathbf{B}_{exch}|$ is expected to depend crucially on the overlap between the graphene π-orbitals with the iron d-orbitals of the FMI. One can readily assume that the regions where the electrodes are on top of the graphene experience a different strength of the exchange field than regions where the graphene lies freely on the surface.

Our analysis can be further extended to the spin transport modulation dependencies shown in figures 4(b)–(d). Figure 5(b) shows the modulation of the spin signal depending on d. These results can also be fit with $\lambda = 1.8$ μm and $|\mathbf{B}_{exch}| = 0.2$ T. When

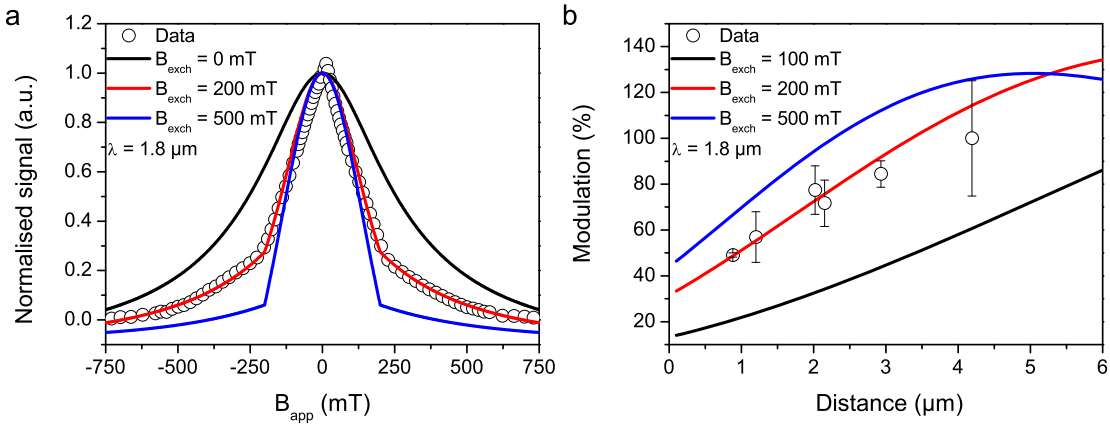

Figure 5. Modelling of the spin transport in the presence of an exchange field in the two different experimental configurations. (a) The standard Bloch spin diffusion model is modified to take the proximity induced exchange field into consideration. The pure spin signal is extracted from the Hanle precession curves and shown with the model for three different exchange field contributions. (b) The modulation of the spin signal originating from the proximity induced exchange field is shown for three different exchange field strengths. In both independent measurements we extract $|\mathbf{B}_{\mathrm{exch}}| \sim 0.2$ T by fitting the data. No fitting is possible for $|\mathbf{B}_{\mathrm{exch}}|$ outside the range of 0.15–0.25 T and λ outside the range of 1.5 –3 μm (see supplementary information).

extrapolating the data to $d = 0$, we find ~35% modulation which can be described with our model:

$$\frac{R_{\mathrm{NL}}^{\max} - R_{\mathrm{NL}}^{\min}}{R_{\mathrm{NL}}^{\max}}|_{d=0} = 1 - \frac{1}{\sqrt{2}} \frac{\sqrt{1 + \sqrt{1 + (\omega\tau_{\mathrm{s}})^2}}}{\sqrt{1 + (\omega\tau_{\mathrm{s}})^2}},$$

where $\omega = \frac{\mathrm{g}}{\hbar}\mu_{\mathrm{B}} |\mathbf{B}_{\mathrm{exch}}|$. Using $|\mathbf{B}_{\mathrm{exch}}| = 0.2$ T, we obtain $\tau_{\mathrm{s}} \sim 40$ ps. Assuming that the spin and charge diffusion (D_{c}) coefficients coincide, we deduce $\lambda = \sqrt{D_{\mathrm{c}}\tau_{\mathrm{s}}} \sim 500$ nm, which resembles the λ extracted from distance dependent spin signal, again suggesting an inhomogeneous exchange field.

In summary, we have demonstrated the detection of ferromagnetic exchange field in graphene by spin transport at room temperature, 75 and 4.7 K. The exchange field strength is quantified in two different experimental configurations to be approximately 0.2 T. Given the theoretical results on idealised systems, substantial enhancement should be possible by appropriate interface optimisation [16]. We proposed spin-transport measurements as the most direct way to study the exchange field in graphene. Furthermore, we showed that a spin current can be efficiently modulated by controlling the exchange field, which opens up new directions to control spins in graphene based spintronic devices.

Methods

Our graphene flakes are exfoliated from HOPG graphite crystals (HQ Graphene) on silicon oxide substrates. Single layer graphene flakes are selected by optical contrast and transferred to target substrates with a custom-built transfer stage using a polycarbonate based pickup technique. The commercially available (111) single crystal YIG films (Matesy GmbH) are grown by liquid phase epitaxy with 210 nm YIG thickness on GGG substrates. The films are cleaned with acetone, isopropanol and 180 s in 200 W oxygen plasma to remove organic residues. To minimise water contamination at the interface between graphene and YIG, the substrates are kept for 15 min in a furnace at 500 °C, until the graphene is transferred at 140 °C.

After transfer, the polycarbonate is dissolved in chloroform and the graphene is cleaned for one hour in a furnace at 350 °C in an Ar/H_2 atmosphere. The flake is connected with electrodes made of titanium oxide tunnel barriers (0.8 nm), ferromagnetic cobalt electrodes (45 nm) and an aluminium capping layer (5 nm) using e-beam lithography. The samples are characterised in a cryostat with standard AC-lock-in measurement techniques at room as well as low temperatures. We apply typical AC currents between 1 and 20 μA with frequencies between 1 and 13 Hz. At 75 K the electrodes show a contact resistance of the order of 1–3 kΩ and a spin signal between 7 Ω at 500 nm contact spacing and 10 mΩ at 3.9 μm spacing. Measurements of Shubnikov–de Haas oscillations at $T = 2$ K, reveal a carrier density of the order of 3×10^{12} cm^{-2} and a mobility of 720 cm^2 V^{-1} s^{-1}. In different graphene/YIG samples we observe holes as charge carriers resulting from doping during the transfer process. Further details are discussed in the supplementary information.

Acknowledgments

We acknowledge A Aqeel, P Zomer, M de Roosz and J G Holstein for technical assistance, J Ingla-Aynes and A M Kamerbeek for fruitful discussions. This research has received funding from the European Union's 7th Framework Programme within the Marie Curie initial training network 'Spinograph' (grant 607904), the 'Graphene Flagship' (grant 604391) and the Dutch

'Foundation for Fundamental Research on Matter' (FOM).

Author contributions

BJvW, JCL, AAK and MW conceived the experiments. JCL and AAK designed and carried out the experiments. JCL, AAK and BJvW analysed and discussed the data and wrote the manuscript.

Competing financial interests

The authors declare no competing financial interests.

References

[1] Han W, Kawakami R K, Gmitra M and Fabian J 2014 Graphene spintronics *Nat. Nanotechnol.* **9** 794–807

[2] Roche S *et al* 2015 Graphene spintronics: the European flagship perspective *2D Mater.* **2** 30202

[3] Nair R R *et al* 2012 Spin-half paramagnetism in graphene induced by point defects *Nat. Phys.* **8** 199–202

[4] McCreary K M, Swartz A G, Han W, Fabian J and Kawakami R K 2012 Magnetic moment formation in graphene detected by scattering of pure spin currents *Phys. Rev. Lett.* **109** 186604

[5] Giesbers A J M *et al* 2013 Interface-induced room-temperature ferromagnetism in hydrogenated epitaxial graphene *Phys. Rev. Lett.* **111** 166101

[6] Yazyev O V and Helm L 2007 Defect-induced magnetism in graphene *Phys. Rev.* B **75** 1–5

[7] Baringhaus J *et al* 2014 Exceptional ballistic transport in epitaxial graphene nanoribbons *Nature* **506** 349–54

[8] Magda G Z *et al* 2014 Room-temperature magnetic order on zigzag edges of narrow graphene nanoribbons *Nature* **514** 608–11

[9] Wang Z, Tang C, Sachs R, Barlas Y and Shi J 2015 Proximity-induced ferromagnetism in graphene revealed by the anomalous Hall effect *Phys. Rev. Lett.* **114** 16603

[10] Semenov Y G, Kim K W and Zavada J M 2007 Spin field effect transistor with a graphene channel *Appl. Phys. Lett.* **91** 39–42

[11] Haugen H, Huertas-Hernando D and Brataas A 2008 Spin transport in proximity-induced ferromagnetic graphene *Phys. Rev.* B **77** 115406

[12] Yang H *et al* 2013 Proximity effects induced in graphene by magnetic insulators: first-principles calculations on spin filtering and exchange-splitting gaps *Phys. Rev. Lett.* **110** 46603

[13] Swartz A G *et al* 2012 Integration of the ferromagnetic insulator EuO onto graphene *ACS Nano* **6** 10063–9

[14] Wei P *et al* 2016 Strong interfacial exchange field in the graphene/EuS heterostructure *Nat. Mater.* **15** 711–6

[15] Mendes J B S *et al* 2015 Spin-current to charge-current conversion and magnetoresistance in a hybrid structure of graphene and yttrium iron garnet *Phys. Rev. Lett.* **115** 226601

[16] Hallal A *et al* 2016 Tailoring magnetic insulator proximity effects in graphene: first-principles calculations arXiv:1610.09554

[17] Jedema F J, Heersche H B, Filip A T, Baselmans J J A and van Wees B J 2002 Electrical detection of spin precession in a metallic mesoscopic spin valve *Nature* **416** 713–6

[18] Popinciuc M *et al* 2009 Electronic spin transport in graphene field-effect transistors *Phys. Rev.* B **80** 214427

[19] Tombros N, Jozsa C, Popinciuc M, Jonkman H T and van Wees B J 2007 Electronic spin transport and spin precession in single graphene layers at room temperature *Nature* **448** 571–4

[20] Guimarães M H D *et al* 2014 Controlling spin relaxation in hexagonal BN-encapsulated graphene with a transverse electric field *Phys. Rev. Lett.* **113** 1–5